Chapter 1

Comparative Antibacterial Effects of a Novel Copper and Silver-Based Core/Shell Nanostructure by Sonochemical Method

Selcan Karakus, Ezgi Tan, Merve Ilgar,
Ismail Sıtkı Basdemir and Ayben Kilislioglu

Additional information is available at the end of the chapter

http://dx.doi.org/10.5772/intechopen.81588

Abstract

In this study, the antibacterial effect of novel copper (Cu) and silver (Ag) metal-based core-shell nanostructures against *Escherichia coli* (*E. coli*-Gram negative) was investigated. The novel copper- and silver-based nanostructures were prepared separately by using nontoxic, biodegradable, and biocompatible biopolymers chitosan and guar gum-polyvinyl alcohol (GG-PVA), which were modified by inorganic phases SiO_2 and sepiolite. On the other hand, guar gum-PVA (GG-PVA) was modified by sepiolite, and this nanostructure was prepared only for silver. Besides, Cu was dispersed in a different biopolymer chitosan by sonochemical method in the presence and absence of SiO_2. X-ray photoelectron spectroscopy (XPS), scanning electron microscopy (SEM), and X-ray diffraction (XRD) techniques were used to characterize the surface chemistry and morphology of the core/shell nanostructure. Nanoscale zero-valent Cu (NZVCu) was found under thin CuO film according to the XPS results. SEM images showed that spherical Cu/CuO@SiO_2 nanostructures (~100 nm) were homogenously dispersed in the chitosan by using sonochemical method. Antibacterial property of the core-shell nanostructures was analyzed by well-diffusion method against *Escherichia coli* (*E. coli*-Gram negative). Cu/CuO@SiO_2 nanostructures were found very effective against the *E. coli* due to high ratio of NZVCu in the nanostructure.

Keywords: sonochemistry, chitosan, silica, core-shell nanostructure, guar gum

1. Introduction

Nanostructures are novel materials obtained by dispersing a small amount of nano-sized filler into a biopolymer matrix while preserving the material biodegradability and nontoxicity [1]. Depending on the dispersion and size of the inorganic filler component in nanostructures, they can exhibit improved mechanical, physical, chemical, and barrier properties, and biological reactivity in comparison to pure biopolymers. Because of their nanometer-size dispersion, biopolymer-clay nanocomposites exhibit large-scale advances in the mechanical and physical properties compared with pure biopolymers [2]. Generally, nanoparticles are prepared by chemical reduction, co-precipitation, sol-gel method, hydrothermal synthesis, thermal reduction, microwave process, vacuum vapor deposition, and sonochemical method [3–6].

The metal core-shell nanoparticle has many significant usages such as particle separation, drug delivery, magnetic resonance imaging, Raman imaging, and biosensor applications [7]. Various multicomponent heterostructured metallic nanoparticles are widely used as antibacterial agents (zinc oxide (ZnO), silver (Ag), Ag@ SiO_2, iron (Fe), molybdenum oxide (MoO_3), cerium oxide nanoparticles (CeO_2), gold-silver (Au-Ag), zirconium oxide ZrO_2, aluminum oxide (Al_2O_3), and magnesium oxide (MgO)) [8–17]. Rai et al. showed that nanomaterial load, type of substance, size and shape of nanoparticles, surface functional groups, crystallinity concentration are significant factors for their antibacterial effects. In spite of the advantages, their toxicity and safety are barriers that limit their efficient and safe use [18]. Dizaj et al. explained that there are two approaches that explain the antibacterial effect of metal nanoparticles: (a) free metal ion and (b) oxidative stress [19].

The copper-based nanoparticles are preferred to gold or silver nanoparticles because of low cost; high surface area; good thermal, mechanical stability, antimicrobial activity, and UV-light barrier property; high-performance conductive material in various applications; and use in photovoltaic and photocatalytic fields owing to their narrow band gap (1.2 eV) [20–25].

Chakraborty et al. evidenced that the antibacterial role of the Cu(II) oxide nanoparticle was a "particle-specific effect" which caused cellular DNA damage through phospho-di-ester bond breakage [26]. Gomes et al. demonstrated that Cu-salts were more toxic than Cu-NPs because of the oxidative stress and differential gene expression [27]. Wahid et al. underlined that copper-based nanostructures are easily released out of human body and can be easily mixed with polymers [28]. Gotzmann et al. pointed out that *Bacillus subtilis* is more sensitive to copper, but *E. coli* and *Staphylococcus aureus* are more sensitive to silver and discovered that the silver/copper blend displayed interdependent forceful antibacterial property [29]. Lv et al. provided antibacterial Cu nanoparticle (dosage of 100 g/mL) for disinfection of drinking water. They explained that cell of *Escherichia coli* were killed because of the reactive oxygen species with H_2O_2 playing a key role [30].

Chitosan is a natural aminopolysaccharide, nontoxic, biocompatible, biodegradable, derived by the deacetylation of chitin, and widely preferred in the biocomposite material preparation processes [31–34]. It has antibacterial property in an acidic solution depending on the kind of chitosan, molecular weight, and the degree of polymerization [35, 36]. Tamayo et al. reported that the -OH and $-NH_2$ groups of chitosan can react with H^+ ions to generate protonized

chitosan with -NH^{3+} functional groups in acetic acid medium. The size and shape of nanoparticles are associated with protonized -NH_3^+ chitosan on surfaces and it decreases the amount of agglomeration, so we can synthesize more stable nanostructure [37, 38]. In this study, we determined that the most important condition is to control the size of nanoparticle which increases owing to self-agglomeration and can be intercepted by the addition of chitosan. The chemical bonds (Si-O-Si bonds) on the silica surface are unsaturated because the surface is active during synthesis. When silica functionalized with chitosan, the NH_2-functional shell was covalently bounded to the surfaces of silica and the reducing ability of SiO_2 increased when functionalized with amino groups [39, 40].

Our hypothesis in this study is acoustic cavitation, and critical amount of the inorganic phase played a key role in synthesizing Chi/Cu/CuO@SiO_2 core-shell nanostructure via sonochemistry. These cavitations live through couple of cycles of the ultrasound medium and collapse in a few nanoseconds because of high-temperature (>1000 K) and pressure (>100 atm) conditions in the solution. The chemical bonds (Si-O-Si bonds) on the silica surface are unsaturated because the surface is reactive during the synthesis. When silica functionalized with chitosan, the NH_2-functional shell was attached via H-bonds to the surface of silica and the reducing ability of SiO_2 increased when functionalized with amino groups. SiO_2 was very effective in reduction of Cu^{2+} into elemental copper. We prepared nanostructures with unique antibacterial properties to destroy pathogenic microorganisms by using sonochemical method. Our aim was the synthesis of the novel core-shell nanoparticle which affects the rate of microbial growth at very low concentrations and produces free radicals (superoxide ($^{\cdot}O^{2-}$), hydroxyl radical ($^{\cdot}OH$), hydrogen peroxide (H_2O_2)) [41–45]. The well-diffusion method was used to determine the antibacterial activity against pathogen bacteria such as *Escherichia coli*. The growth inhibition zones appeared in the agar layer. We found that the mechanism is founded on self-assembly reduction/oxidation reactions that occur among copper, SiO_2, and chitosan.

Silver is commonly used as a well-known antibacterial additive in polymer blends for food packaging and bionanotechnology applications. Guar gum is a biodegradable and eco-friendly biopolymer and is formed of mannose and galactose units [46]. Poly(vinyl alcohol) (PVA) is mixed with guar gum through hydrogen bonds and also has biocompatibility, biodegradability, and good mechanical properties [47]. In this study, Ag@Sepiolite-based nanostructure was encapsulated in a PVA/guar gum/matrix. Antibacterial property of the copper and silver core-shell nanostructures was analyzed by well-diffusion method against *Escherichia coli* (*E. coli*-Gram negative). Cu/CuO@SiO_2 nanostructures were found to be very effective against the *E. coli* due to high ratio of NZVCu in the nanostructure. According to this research, the major role of silica in Cu-based core-shell nanostructures under ultrasonic effect was highlighted.

2. Experimental

2.1. Materials

Chitosan (low molecular weight) and cetyltrimethylammonium bromide (CTAB) were purchased from Sigma-Aldrich. Glacial acetic acid, sodium hydroxide, $AgNO_3$, silica gel, $NaBH_4$,

and Copper(II) sulfate pentahydrate ($CuSO_4.5H_2O$) were purchased from Merck. In the experimental setup, all chemicals and reagents were analytical grade and used without further purification.

2.2. Preparation of the Cu core-shell nanostructure

Chitosan aqueous solutions of low molecular weight, 0.02 g (100 mL), were prepared by dissolving chitosan powder in 5% (v/v) glacial acetic acid. The homogenous solution was obtained by continuous mixing at 25°C. Solutions containing 0.01 M $CuSO_4.5H_2O$ and 0.02 M $NaBH_4$were prepared separately in a 10-mL deionized water and mixed with a magnetic stirrer drop by drop. Silica gel of weight 0.02 g was added. Then, they were sonicated for 15 minutes (20 kHz) with chitosan solutions under a nitrogen atmosphere by using a Bandelin SONOPULS homogenizer. The samples were dried at 45°C to a constant weight (**Figure 1**).

2.3. Preparation of the Ag core-shell nanostructure

Natural sepiolite of weight 5 g was stirred using 500-mL distilled water to remove the soluble impurities for 1 night. Cetyltrimethylammonium bromide (CTAB) of weight 2 g in 100 mL hot distilled water was added into sepiolite solution and was mixed for 24 hour. Then, the samples were dried overnight at 110°C to a constant weight.

Sepiolite/CTAB of weight 0.0025 g was added to each polymer solution, and they were sonicated for 5 minutes. Solution of 0.133 M, 2.5 mL $NaBH_4$ was added drop by drop to 0.133 M,

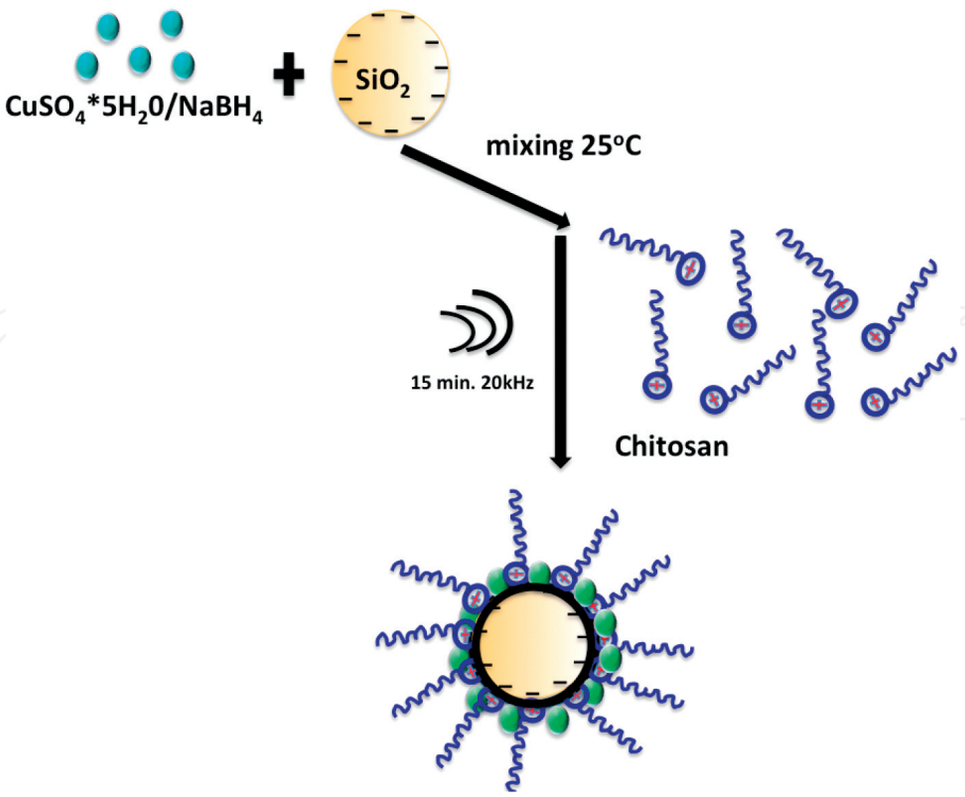

Figure 1. The mechanism of Chi/Cu/CuO@SiO_2 core-shell nanostructure.

http://dx.doi.org/10.5772/intechopen.81588

2.5 mL $AgNO_3$ under nitrogen atmosphere while it was sonicated. Reduced Ag solution was added drop by drop to each PVA/Guar Gum polymer mixture (1:1) for 5 minutes under sonication under N_2 atmosphere. All samples were dried at 60°C. Also, the experiments were carried out without Ag and sepiolite/CTAB.

2.4. Characterization of core-shell nanostructure

2.4.1. X-ray diffraction (XRD) study

The diffraction patterns of the core/shell nanostructure were analyzed by XRD diffractometer (XRD, PAN analytical Xpert-Pro, Cu Ka: 1.5406 Å, a nickel monochromator filtering wave at 40 kV and 40 mA, with a 0.4/min at room temperature, Bruker D8 Advance X-ray Diffractometer).

2.4.2. Scanning electron microscopy (SEM)

The morphological studies were conducted using a Jeol/eo version 1.0 instrument Jsm6390 scanning electron microscope (SEM). The samples were coated with platinum before SEM analysis.

3. Results and discussion

3.1. XRD results

Figure 2 presents the XRD patterns of Chi/Cu/CuO@SiO_2, Chi/Cu/CuO, chitosan, and SiO_2. SiO_2 not only plays a key role in the reduction of copper salt into metallic copper during sonication-assisted mixing of inorganic and organic phases but also leads to the formation of a mineral. According to the XRD results, the diffraction data obtained were well matched with dioptase mineral (ICSD 100077 and PDF 33–487). The XRD pattern of nanostructure indicates the presence of Cu/CuO on the surface of SiO_2. A simple scheme was drawn to demonstrate the nanostructure (**Figure 3**). The XRD pattern of copper displayed characteristic peaks at 2 theta of 22.8, 24.3, 31.5, 34.0, 38.7, 48.9, 53.4, 58.0, 61.0, 66.1, 67.9, 72.2, and 74.9°, respectively [23].

Figure 4 presents the XRD patterns of (a) PVA-Guar Gum (b) PVA-Guar Gum-Sepiolite (c) PVA-Guar Gum Ag@Sepiolite core-shell nanoparticle. The XRD pattern of silver displayed characteristic peaks at 2 theta of 38.19, and 44.26°, respectively.

3.2. SEM results

According to the SEM images of the core-shell nanostructure, a homogenous structure was obtained by using sonication method. The SEM micrographs and EDAX mapping of Cu are shown in **Figures 5** and **6**.

3.3. X-ray photoelectron spectroscopy analysis

The high-resolution XPS spectra of the Chi/Cu/CuO, Chi/Cu/CuO@SiO_2 nanostructures for the copper regions are presented in **Figure 7**. The intensities of spectra of same elements can be compared with each other in both samples. For the Chi/Cu/CuO@SiO_2 sample, elemental Cu shows $2p_{3/2}$ peak positioned at 933.6 eV and $2p_{1/2}$ peak positioned at 953.4 eV with no satellite.

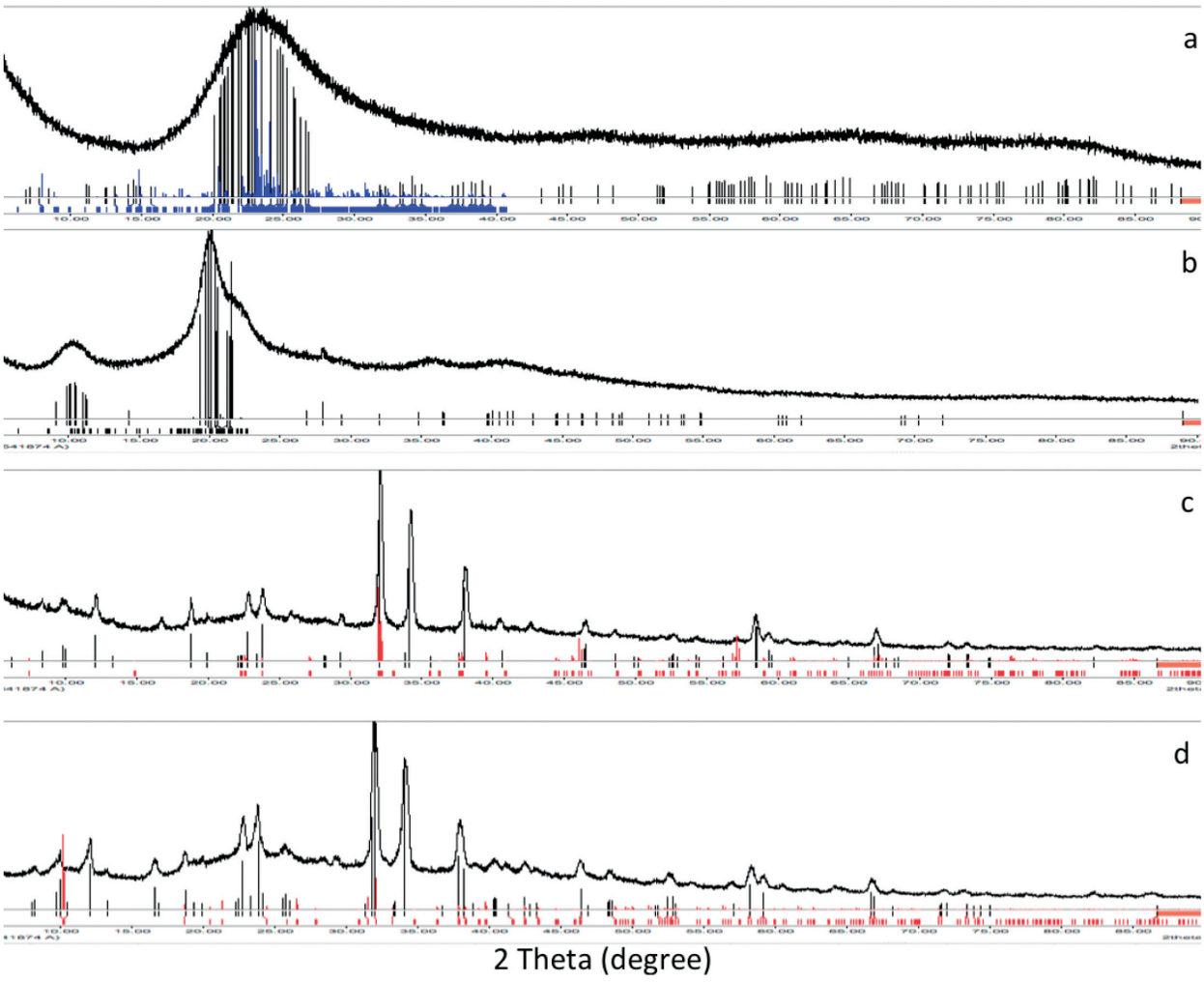

Figure 2. XRD patterns of (a) Chitosan (b) SiO_2 (c) Chi/Cu/CuO (d) Chi/Cu/CuO@SiO_2.

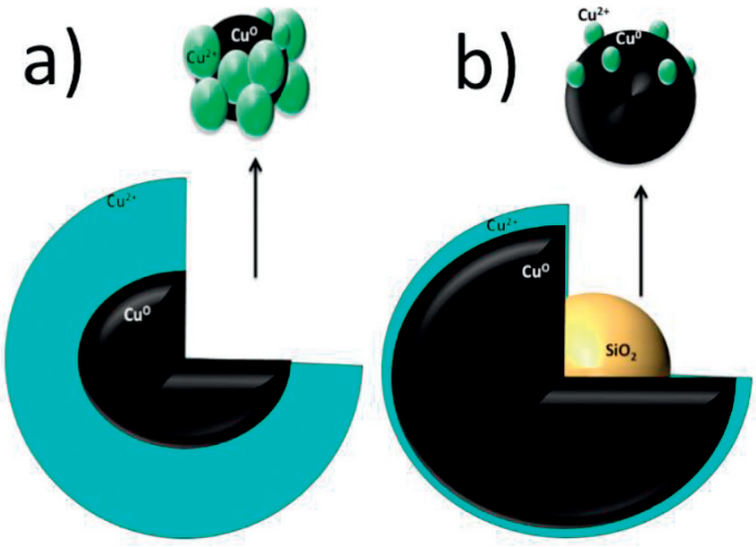

Figure 3. (a) Chi/Cu/CuO core-shell nanoparticle (b) Chi/Cu/CuO@SiO_2 core-shell nanoparticle.

http://dx.doi.org/10.5772/intechopen.81588

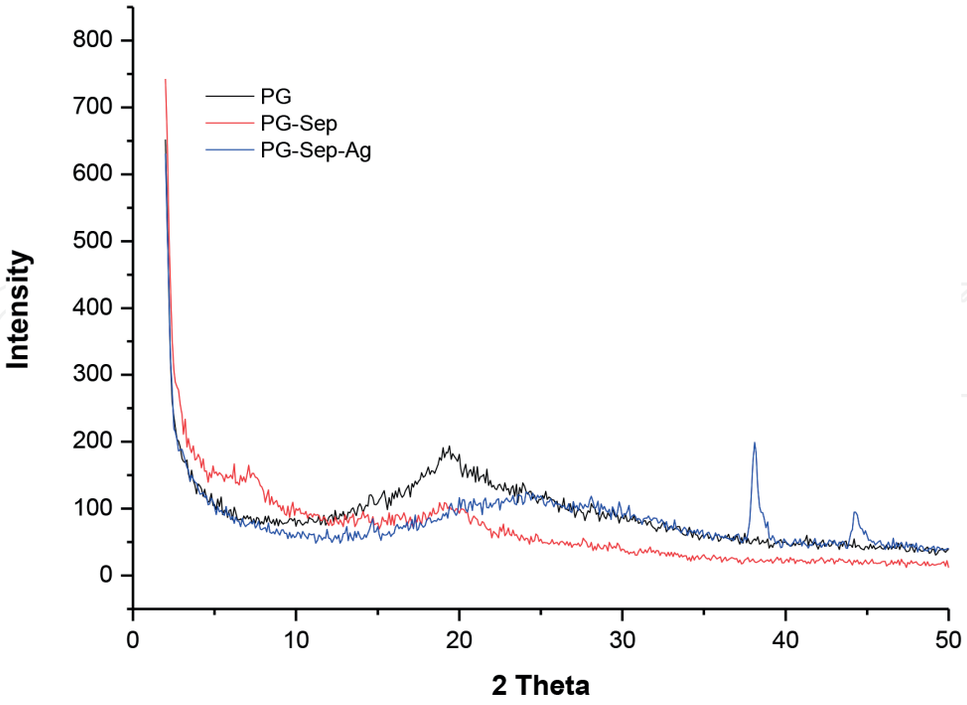

Figure 4. XRD patterns of (a) PVA-Guar Gum (b) PVA-Guar Gum-Sepiolite (c) PVA-Guar Gum Ag@Sepiolite core-shell nanoparticle.

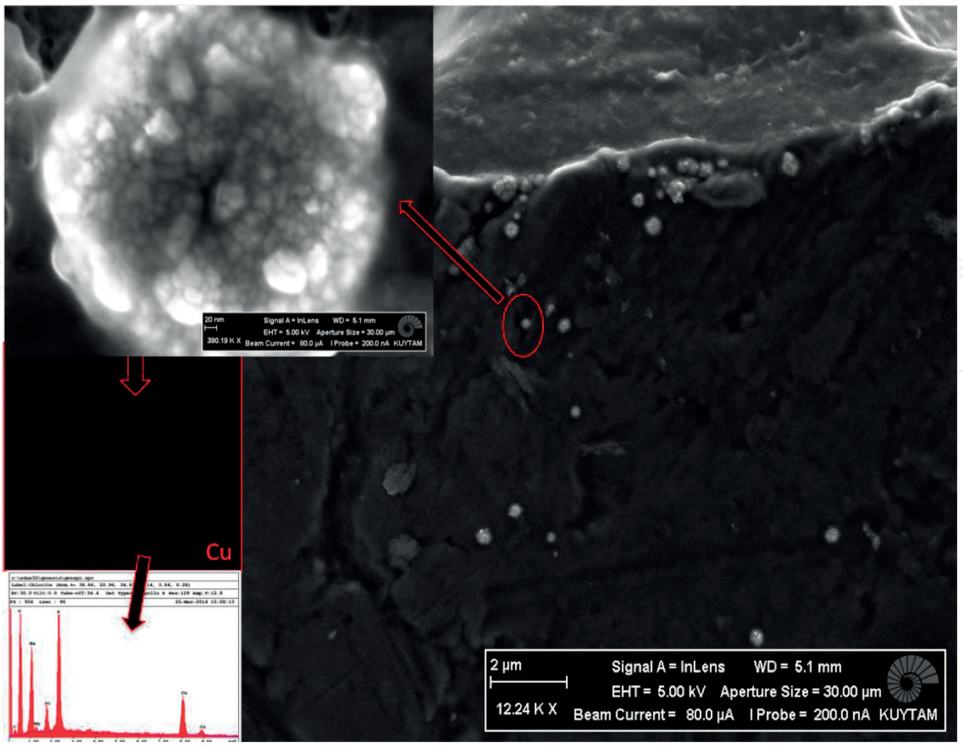

Figure 5. SEM images of the surface of Chi/Cu/CuO@SiO_2.

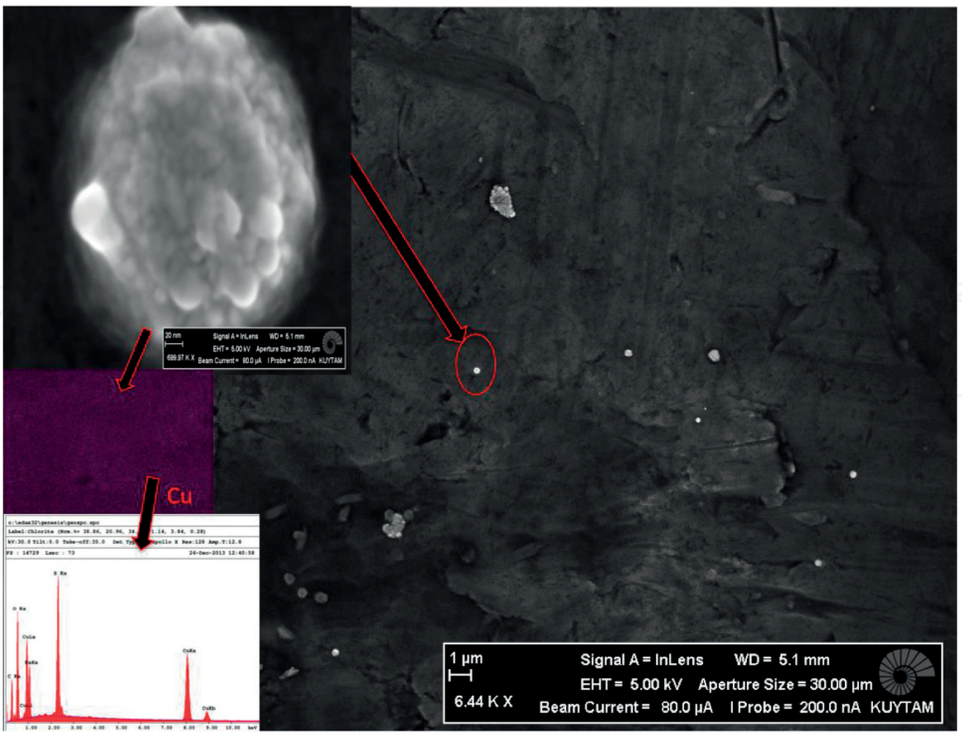

Figure 6. SEM images of the surface of Chi/Cu/CuO.

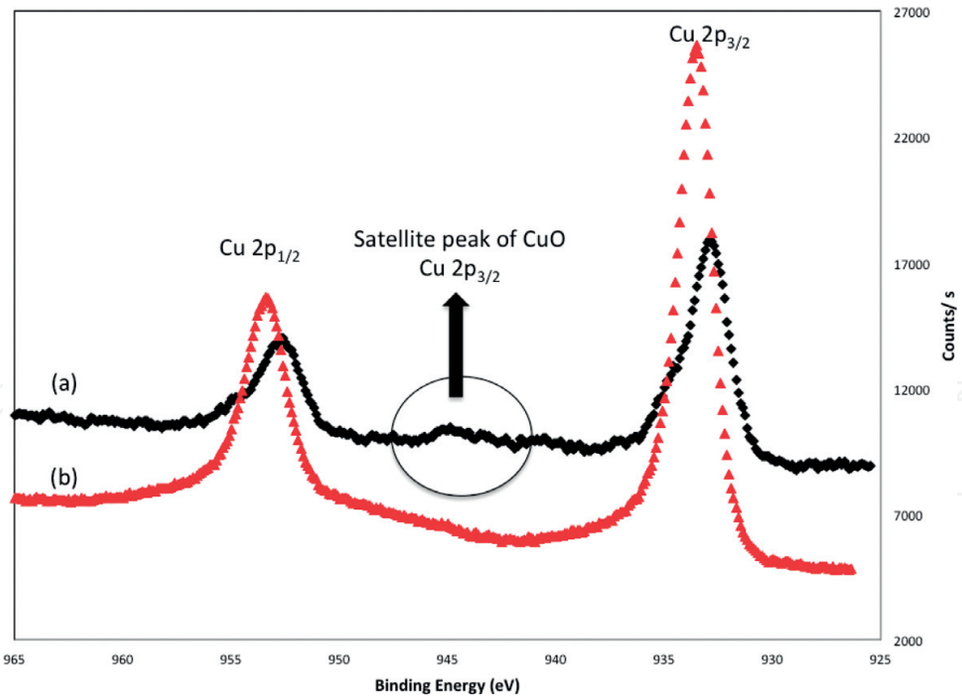

Figure 7. XPS pattern of (a) Chi/Cu/CuO (b) Chi/Cu/CuO@SiO_2.

For the Chi/Cu/CuO sample, the $2p_{3/2}$ maximum peak was positioned at 932.8 eV and $2p_{1/2}$ peak positioned at 952.5 eV. A satellite peak identifies the species as CuO due to surface oxidation of the ZVCu nanoparticles.

http://dx.doi.org/10.5772/intechopen.81588

3.4. Antibacterial activity of the core-shell nanoparticle

The Gram-negative *Escherichia coli* bacteria (NCTC 10538) were cultured at 37°C on a shaking incubator and prepared by spreading of test organism on blood-enriched Mueller-Hinton agar, adjusting 10 mg of sample. The petri dishes were incubated to 35°C at 24 hours (180 rpm). The petri dishes were analyzed for the presence of a clear zone of inhibition. The antibacterial agents inhibited pathogenic bacteria growth leading to a clear, isolated zone in the petri dish. The power of antibacterial properties is proportional to the diameter of inhibition zone (disk diffusion). **Figure 8** shows a clear inhibition zone against *E. coli* microorganisms. The diameter of inhibition zone for nanoparticle against *E. coli* is approximately 20 mm, so that Chi/Cu/CuO@SiO_2 has increased antibacterial performance against the bacteria. **Figure 9** shows that the diameter of inhibition zone for nanoparticle against *E. coli* is approximately 5 mm, so that PVA-Guar Gum Ag@Sepiolite has antibacterial property against the bacteria. Experimental results

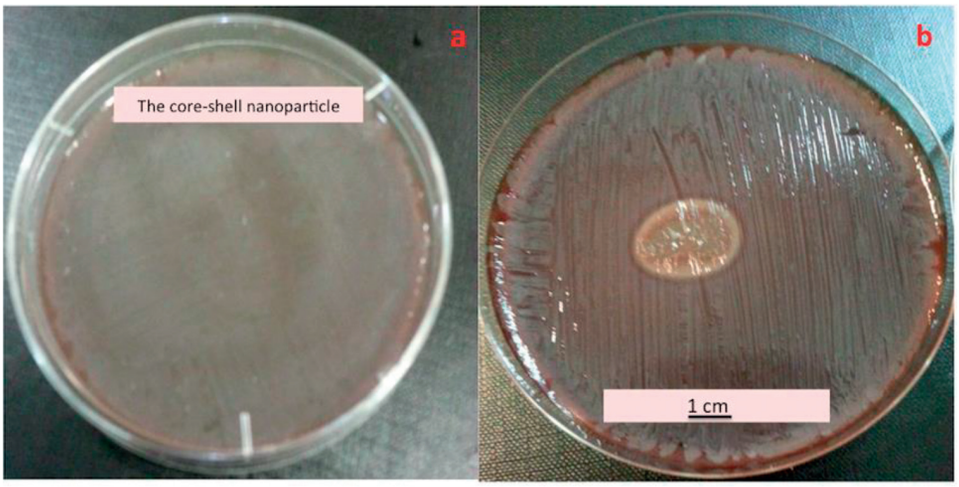

Figure 8. The zone of inhibition covered by Chi/Cu/CuO@SiO_2 nanoparticles against *E. coli*. (a) 1 hour; (b) 24 hours.

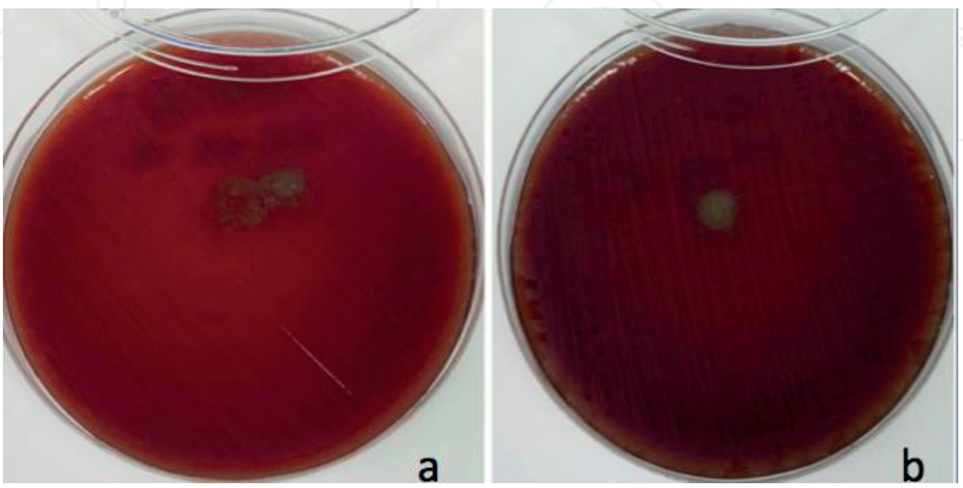

Figure 9. The zone of inhibition covered by PVA-Guar Gum Ag@sepiolite nanoparticles against *E. coli*. (a) 1 hour; (b) 24 hours.

showed that the size of nanoparticle, amount of nanoparticle, the oxidative stress, and particle-specific effect of SiO_2 are responsible factors for their improved antibacterial effect [45].

4. Conclusion

A novel antibacterial core/shell nanostructure was prepared by using chitosan which was modified by SiO_2 and Cu. Cu was dispersed in chitosan by sonochemical method in the presence and absence of SiO_2. When sonication was applied during preparation, the critical amount of SiO_2 and Cu caused the formation of dioptase mineral. SiO_2 led to the reduction in copper salt into metallic copper during dispersion by sonication and also produced a dioptase mineral.

The specific advantages of the preparation of this novel Cu/CuO@SiO_2 core/shell nanostructure included: (i) a low-cost, simple, convenient, and easily feasible sonochemical method, (ii) high content of Cu(0) nanoparticle in the targeting antibacterial agent, (iii) the novel nanoparticle has high bactericidal capacity, and (iv) critical mass production of the antibacterial core-shell nanoparticle. According to the results of the analysis, one could say that the copper-based nanostructure was found more effective against *E. coli* than the silver-based nanostructure due to the major role of silica in Cu-based core-shell nanostructures by using sonochemical method.

Acknowledgements

This work was supported by the research fund of Istanbul University project number 13145. The authors acknowledge the support on SEM and XPS analysis from Koc University Surface Science and Technology Center (KUYTAM).

Author details

Selcan Karakus*, Ezgi Tan, Merve Ilgar, Ismail Sıtkı Basdemir and Ayben Kilislioglu

*Address all correspondence to: selcan@istanbul.edu.tr

Department of Chemistry, Faculty of Engineering, Istanbul University-Cerrahpasa, Istanbul, Turkey

References

[1] Bordes P, Pollet E, Avérous L. Nano-biocomposites: Biodegradable polyester/nanoclay systems. Progress in Polymer Science. 2009;**34**:125-155

[2] Ke T, Le Y, Wang JX, Chu GW, Chen JF, Shao L. Cu nanoparticle preparation in a tube-in-tube microchannel reactor and encapsulation by silica. Materials Letters. 2010;**64**: 1717-1719

[3] Chowdhury MNK, Beg MDH, Khan MR, Mina MF. Synthesis of copper nanoparticles and their antimicrobial performances in natural fibres. Materials Letters. 2013;**98**:26-29

[4] Im HJ, Jung EC. Colloidal nanoparticles produced from Cu metal in water by laser ablation and their agglomeration. Radiation Physics and Chemistry. 2016;**118**:6-10

[5] Antonoglou O, Giannousi K, Arvanitidis J, Mourdikoudis S, Pantazaki A, Dendrinou-Samara C. Elucidation of one step synthesis of PEGylated CuFe bimetallic nanoparticles. Antimicrobial activity of CuFe@PEG vs Cu@PEG. Journal of Inorganic Biochemistry. 2017;**177**: 159-170

[6] Salavati-Niasari M, Hosseinzadeh G, Davar F. Synthesis of lanthanum hydroxide and lanthanum oxide nanoparticles by sonochemical method. Journal of Alloys and Compounds. 2011;**509**:4098-4103

[7] Chen Y, Wang Z, Chen X, Zeng D, Li M, Peng DL. Solution preparation of alloy core-shell nanoparticles: The case of Ni-Cu@Au-Cu nanoparticles. Materials Letters. 2013;**99**:180-183

[8] Joe A, Park SH, Shim KD, Kim DJ, Jhee KH, Lee HW, et al. Antibacterial mechanism of ZnO nanoparticles under dark conditions. Journal of Industrial and Engineering Chemistry. 2017;**45**:430-439

[9] Alimunnisa J, Ravichandran K, Meena KS. Synthesis and characterization of Ag@SiO_2 core-shell nanoparticles for antibacterial and environmental applications. Journal of Molecular Liquids. 2017;**231**:281-287

[10] Asghara MA, Zahir E, Shahid SM, Khan MN, Asghar MA, Iqbal J, et al. Iron, copper and silver nanoparticles: Green synthesis using green and black tea leaves extracts and evaluation of antibacterial, antifungal and aflatoxin B1 adsorption activity. LWT - Food Science and Technology. 2018;**90**:98-107

[11] Najafi M, Abbasi A, Masteri-Farahani M, Janczak J. Sonochemical preparation of bimetallic (Cu/Mo) oxide nanoparticles as catalysts for dye degradation under mild conditions. Polyhedron. 2015;**93**:76-83

[12] Gopinathan E, Viruthagiri G, Shanmugam N, Sathiya Priya S. Optical, surface analysis and antibacterial activity of ZnO-CuO doped cerium oxide nanoparticles. Optik. 2015;**126**: 5830-5835

[13] Yu X, Li J, Shi T, Cheng C, Liao G, Fan J, et al. A green approach of synthesizing of Cu-Ag core-shell nanoparticles and their sintering behavior for printed electronics. Journal of Alloys and Compounds. 2017;**724**:365-372

[14] Banerjee M, Sharma S, Chattopadhyay A, Ghosh SS. Enhanced antibacterial activity of bimetallic gold-silver core-shell nanoparticles at low silver concentration. Nanoscale. 2011;**3**:5120-5125

[15] Zhang Y, Wang L, Xu Y. ZrO_2 solid superacid porous shell void TiO_2 coreparticles (ZVT) polyvinylidene fluoride (PVDF) composite membranes with anti-fouling performance for sewage treatment. Journal of Membrane Science. 2015;**260**:258-268

[16] Ansari MA, Khan HM, Khan AA, Cameotra SS, Saquib Q, Musarrat J. Interaction of Al_2O_3 nanoparticles with *Escherichia coli* and their cell envelope biomolecules. Journal of Applied Microbiology. 2014;**116**:772-783

[17] Tang ZX, Lv BF. MgO nanoparticles as antibacterial agent: Preparation and activity. Brazilian Journal of Chemical Engineering. 2014;**31**:591-601

[18] Rai M, Ingle AP, Pandit R, Paralikar P, Gupta I, Chaud MV, et al. Broadening the spectrum of small-molecule anti bacterials by metallic nanoparticles to overcome microbial resistance. International Journal of Pharmaceutics. 2017;**532**:139-148

[19] Dizaj SM, Lotfipour F, Barzegar-Jalali M, Zarrintan MH, Adibkia K. Antimicrobial activity of the metals and metal oxide nanoparticles. Materials Science and Engineering: C. 2014; **44**:278-284

[20] Shankar S, Rhim JW. Effect of copper salts and reducing agents on characteristics and antimicrobial activity of copper nanoparticles. Materials Letters. 2014;**132**:307-311

[21] Ghasemi N, Jamali-Sheini F, Zekavati R. CuO and Ag/CuO nanoparticles: Biosynthesis and antibacterial properties. Materials Letters. 2017;**196**:78-82

[22] Li J, Shi T, Feng C, Liang Q, Yu X, Fan J, et al. The novel Cu nanoaggregates formed by 5 nm Cu nanoparticles with high sintering performance at low temperature. Materials Letters. 2018;**216**:20-23

[23] Oun AA, Rhim JW. Carrageenan-based hydrogels and films: Effect of ZnO and CuO nanoparticles on the physical, mechanical, and antimicrobial properties. Food Hydrocolloids. 2017;**67**:45-53

[24] Gutiérreza MF, Malaquiasa P, Matosa TP, Szesza A, Souzaa S, Bermudeza J, et al. Mechanical and microbiological properties and drug release modeling of an etch-and-rinse adhesive containing copper nanoparticles. Dental Materials. 2017;**33**:309-320

[25] Reddy KR. Green synthesis, morphological and optical studies of CuO nanoparticles. Journal of Molecular Structure. 2017;**1150**:553-557

[26] Chakraborty R, Sarkar RK, Chatterjee AK, Manju U, Chattopadhyay AP, Basu T. A simple, fast and cost-effective method of synthesis of cupric oxide nanoparticle with promising antibacterial potency: Unraveling the biological and chemical modes of action. Biochimica et Biophysica Acta. 2015;**1850**:845-856

[27] Gomes SIL, Murphy M, Nielsen MT, Kristiansen SM, Amorim MJB, Scott-Fordsmand JJ. Cu-nanoparticles ecotoxicity—Explored and explained? Chemosphere. 2015;**139**:240-245

[28] Wahid F, Wang HS, Lu YS, Zhong C, Chu LQ. Preparation, characterization and antibacterial applications ofcarboxymethyl chitosan/CuO nanocomposite hydrogels. International Journal of Biological Macromolecules. 2017;**101**:690-695

[29] Gotzmann G, Jorsch C, Wetzel C, Funk HWR. Antimicrobial effects and dissolution properties of silver copper mixed layers. Surface and Coating Technology. 2018;**336**: 22-28, article in press. DOI: 10.1016/j.surfcoat.2017.09.036

[30] Lv Q, Zhang B, Xing X, Zhao Y, Cai R, Wang W, et al. Biosynthesis of copper nanoparticles using Shewanella loihica PV-4with antibacterial activity: Novel approach and mechanisms investigation. Journal of Hazardous Materials. 2018;**347**:141-149

[31] Pillai CKS, Paul W, Sharma CP. Chitin and chitosan polymers: Chemistry, solubility and fiber formation. Progress in Polymer Science. 2009;**34**:641-678

[32] Chandy T, Sharma CP. Chitosan—as a biomaterial. Biomaterials, Artificial Cells, and Artificial Organs. 1990;**18**:1-24

[33] Paul W, Sharma CP. Chitosan, a drug carrier for the 21st century: A review. STP Pharma Sciences. 2000;**10**:5-22

[34] Muzzarelli RAA, Muzzarelli C. Chitosan chemistry: Relevance to the biomedical sciences. Advances in Polymer Science. 2005;**186**:151-209

[35] Qi L, Xu Z, Jiang X, Hu C, Zou X. Preparation and antibacterial activity of chitosan nanoparticles. Carbohydrate Polymers. 2004;**339**:2693-2700

[36] Sotelo-Boyás ME, Correa-Pacheco ZN, Bautista-Baños S, Corona-Rangel ML. Physicochemical characterization of chitosan nanoparticles and nanocapsules incorporated with lime essential oil and their antibacterial activity against food-borne pathogens. LWT - Food Science and Technology. 2017;**77**:15-20

[37] Tamayo L, Azócar M, Kogan A, Riveros M, Páez M. Copper-polymer nanocomposites: An excellent and cost-effective biocide for use on antibacterial surfaces. Materials Science & Engineering C: Materials for Biological Applications. 2016;**69**:1391-1409

[38] Javed R, Ahmed M, ul Haq I, Nisa S, Zia M. PVP and PEG doped CuO nanoparticles are more biologically active: Antibacterial, antioxidant, antidiabetic and cytotoxic perspective. Materials Science and Engineering: C. 2017;**79**:108-115

[39] Guan Z, Shu Y, Maa Y, Wan J. Factors affecting the physicochemical properties of the modified core/shell NH_2-SiO_2@NZVI nanoparticles. Colloids and Surfaces A: Physicochemical and Engineering Aspects. 2015;**482**:18-26

[40] Markova-Deneva I. Infrared spectroscopy investigation of metallic nanoparticles based on copper, cobalt, and nickel synthesized through borohydride reduction method. Journal of Chemical Technology and Metallurgy. 2010;**45**(4):351-378

[41] Dolores R, Raquel S, Adianez GL. Sonochemical synthesis of iron oxide nanoparticles loaded with folate and cisplatin: Effect of ultrasonic frequency. Ultrasonics Sonochemistry. 2015;**23**:391-398

[42] Arakha M, Roy J, Nayak PS, Mallick B, Jha S. Zinc oxide nanoparticle energy band gap reduction triggers the oxidative stress resulting into autophagy-mediated apoptotic cell death. Free Radical Biology & Medicine. 2017;**110**:42-53

[43] Pandey S, Ramontja J. Sodium alginate stabilized silver nanoparticles—silica nanohybrid and their antibacterial. International Journal of Biological Macromolecules. 2016;**93**: 712-723

[44] Raut SS, Kamble SP, Kulkarni PS. Efficacy of zero-valent copper (Cu(0)) nanoparticles and reducing agents for dechlorination of mono chloroaromatics. Chemosphere. 2016;**159**: 359-366

[45] Chen S, Guo Y, Zhong H, Chen S, Li J, Ge Z, et al. Synergistic antibacterial mechanism and coating application of copper/titanium dioxide nanoparticle. Chemical Engineering Journal. 2014;**256**:238-246

[46] Mukherjee S, Mukhopadhyay S, Zafri MZB, Zhana X, Hashim MA, Gupta BS. Application of guar gum for the removal of dissolved lead from wastewater. Industrial Crops and Products. 2018;**111**:261-269

[47] Das T, Yeasmin S, Khatua S, Acharya K, Bandyopadhyay A. Influence of a blend of guar gum and poly(vinyl alcohol) on long term stability, and antibacterial and antioxidant efficacies of silver nanoparticles. RSC Advances. 2015;**5**:54059-54069